J. Anat. (2006) **209**, pp359–367 doi: 10.1111/j.1469-7580.2006.00610.x

Regional variations in the density and arrangement of elastic fibres in the anulus fibrosus of the human lumbar disc

Lachlan J. Smith and Nicola L. Fazzalari

Bone and Joint Research Laboratory, Division of Tissue Pathology, Institute of Medical and Veterinary Science and Hanson Institute, Adelaide, Australia and Department of Pathology, The University of Adelaide, Australia

Abstract

Elastic fibres are critical components of the extracellular matrix in dynamic biological structures that undergo extension and recoil. Their presence has been demonstrated in the anulus fibrosus of the human lumbar intervertebral disc; however, a detailed regional analysis of their density and arrangement has not been undertaken, limiting our understanding of their structural and functional roles. In this investigation we have quantitatively described regional variations in elastic fibre density in the anulus fibrosus of the human L3–L4 intervertebral disc using histochemistry and light microscopy. Additionally, a multiplanar comparison of patterns of elastic fibre distribution in the intralamellar and interlamellar zones was undertaken. Novel imaging techniques were developed to facilitate the visualization of elastic fibres otherwise masked by dense surrounding matrix. Elastic fibre density was found to be significantly higher in the lamellae of the posterolateral region of the anulus than the anterolateral, and significantly higher in the outer regions than the inner, suggesting that elastic fibre density in each region of the anulus is commensurate with the magnitude of the tensile deformations experienced in bending and torsion. Elastic fibre arrangments in intralamellar and interlamellar zones were shown to be architecturally distinct, suggesting that they perform multiple functional roles within the anulus matrix structural hierarchy.

Key words anulus fibrosus; elastic fibres; intervertebral disc; structure–function.

Introduction

The intervertebral disc is composed of three distinct structures: the central, amorphous, highly hydrated, proteoglycan-rich nucleus pulposus; peripherally, the anulus fibrosus; and superiorly and inferiorly, two endplates of hyaline cartilage (Eyre, 1979; Humzah & Soames, 1988). The anulus fibrosus, composed primarily of interstitial collagens type I and II, has a complex hierarchical structure. Collagen fibres are arranged in bundles, in the inner regions travelling between the endplates and in the outer regions directly between the vertebral bodies, arranged at alternating angles of plus and minus ~30° to the transverse plane, in roughly concentric lamellae around the nucleus pulposus (Marchand & Ahmed, 1990). Spaces between lamellae contain an amorphous proteoglycan-rich gel (Szirmai, 1970).

The mechanical function of the anulus fibrosus is two-fold: to provide mobility to the spine by facilitating flexion, extension, lateral bending and twisting; and to resist the radial forces generated by the bulging of the nucleus pulposus under compressive loads (Langrana et al. 1996). Mobility is facilitated through the extension and reorientation of matrix elements (Hickey & Hukins, 1980). The stresses and strains experienced by the anulus are heterogeneous and anisotropic, and variations in the mechanical properties, structure and chemistry of the extracellular matrix reflect this (Eyre, 1979; Cassidy et al. 1989; Ebara et al. 1996; Fujita et al. 1997, 2000; Elliott & Setton, 2001). Variations in collagen and proteogylcan distribution

Correspondence
Lachlan J. Smith, Bone and Joint Research Laboratory, Division of Tissue Pathology, Institute of Medical and Veterinary Science, Frome Road, Adelaide, SA 5000, Australia. T: +61 882223106; F: +61 882223293; E: lachlan.smith@imvs.sa.gov.au

Accepted for publication *26 May 2006*

are widely documented (Bushell et al. 1977; Eyre, 1979; Oegema, 1993; Skaggs et al. 1994); however, similar attention has not been afforded to elastic fibres.

Elastic fibres have been shown to be critical components of many dynamic biological tissues, including lungs, skin, vasculature and many others (Kielty et al. 2002). They influence mechanical properties such as resilience and low strain stiffness, complementing the role of collagen fibres, which impart tensile strength (Karlinsky et al. 1976; Oakes & Bialkower, 1977; Oxlund & Andreassen, 1980; Oxlund et al. 1988; Lee et al. 2001). The chemistry and ultrastructure of elastic fibres are highly tissue-specific. They commonly consist of a core of highly extensible elastin embedded on a scaffold of stiffer, reinforcing microfibrillar glycoproteins consisting primarily of fibrillins (Kielty et al. 2002; Sheratt et al. 2003). They may also exist with a smaller elastin component (elaunin fibres), or purely as bundles of microfibrils (oxytalan fibres), each of these having distinct functional properties (Barros et al. 2002). Several proteoglycans, including decorin, biglycan and versican, are considered to play critical roles in the integration of elastic microfibrils into the surrounding matrix (Kielty et al. 2002). The precise mechanical role of elastic fibres is considered to be a function of their chemistry, ultrastructure, arrangement and collective density relative to other matrix consituents (Ritty et al. 2002).

The distribution of elastic fibres in the human anulus fibrosus has been examined in a number of qualititative histological studies, at both the light microscopical and the ultrastructural levels (Buckwalter et al. 1976; Hickey & Hukins, 1981; Johnson et al. 1982, 1985; Akhtar et al. 2005a,b; Yu et al. 2005) and it has been suggested that they may play an important mechanical role (Humzah & Soames, 1988). They appear to have multiple distinct patterns of distribution: in intralamellar regions they are aligned parallel to the collagen fibril bundles (Buckwalter et al. 1976; Yu et al. 2005); in interlamellar regions their arrangement appears less isotropic (Yu et al. 2005). A recent study has demonstrated that structural cohesion between the collagen bundles in adjacent lamellae is provided by complex linking elements. The authors of this study theorized that these structures may contain elastic fibres, but were unable to differentiate between elastic and collagenous elements (Pezowicz et al. 2006). Greater understanding of both the arrangement of elastic fibres in the anulus and their density relative to other matrix consituents would provide new insights both into their functional roles in the mechanics of healthy discs, and into their roles in the structural changes associated with degenerative disc disease, as the loss of resilience and elasticity provided by elastic fibres is a major contributing factor in tissue ageing and degradation (Kielty et al. 2002).

Our objectives in this investigation were to perform a quantitative histological analysis of regional variations in elastic fibre density in the anulus, and to conduct a multiplanar comparison of patterns of elastic fibre distribution in the intralamellar and interlamellar zones.

Materials and methods

Specimen preparation

Seven human lumbar spines from individuals ranging in age from 16 to 82 years were harvested at autopsy within 24 h of death from the mortuary at the Royal Adelaide Hospital, sealed in plastic and frozen at –80 °C. Prior to disc excision, spines were X-rayed (Faxitron; Hewlett Packard, Palo Alto, CA, USA) and bone mineral density measurements for vertebral bodies superior and inferior to the discs to be analysed were made (QDR-1000; Hologic, Bedford, MA, USA). Spines were thawed at 4 °C and cuts were made using a scalpel in the transverse plane adjacent to the superior and inferior vertebral bodies and endplates, enabling the removal of complete intervertebral discs. All specimens used in this study were harvested from the L3–L4 level. The physical dimensions of each disc were measured using digital calipers. Discs were hemi-sected mid-sagittally and morphologically graded for degenerative condition according to the scheme of Thompson et al. (1990), modified to account for the differing method of disc excision. Tissue was kept moist at all times using phosphate-buffered saline. Specimen details are presented in Table 1.

Histology

Specimens were fixed in 10% buffered formalin, routinely processed (Tissue-Tek VIP 5; Sakura Finetek, Tokyo, Japan) and paraffin embedded. Sections 25–30 μm thick were cut in the transverse and lamellar planes (Fig. 1) using a sledge microtome (Reichert, Germany) and mounted on gelatin-coated microscope slides. Transverse sections were obtained from the mid-sagittal region of the disc.

Table 1 Specimen details

Age	Sex	Disc height (mm)	Disc grade	Superior VB* T-score	Inferior VB T-score
16	M	12	1	0	0
28	M	9	2	−0.6	−0.8
40	F	13	2	0.3	−0.2
54	M	14	2	−3.6	−3.7
66	M	17	3	−4.7	−5.3
76	F	8	3	−2.1	2
82	M	10	3	0.4	−0.4

*VB = vertebral body.

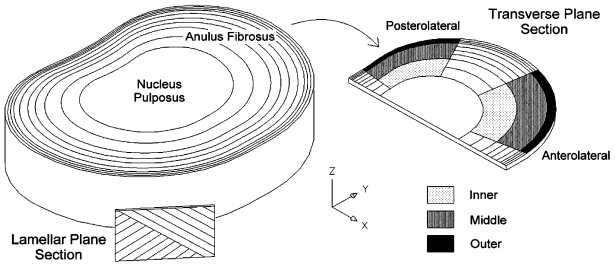

Fig. 1 Schematic representation of the intervertebral disc illustrating section orientations and sampling zones (radial: inner, middle, outer; circumferential: anterolateral, posterolateral).

Sections were baked, brought to distilled water through xylene and a graded series of alcohols, oxidized with 0.5% aqueous potassium permanganate, bleached with 2% oxalic acid, stained using resorcin-fuchsin (Miller's modification, Miller, 1971), dehydrated, cleared in xylene and mounted with DPX. This staining method was selected due to its ability to demonstrate the finest of elastic fibres (Caldini et al. 1990). As negative controls, a subset of sections was incubated in high-purity porcine pancreatic elastase (1 U mL^{-1} in 200 mM Tris-HCl) (Sigma-Aldrich, St Louis, MO, USA) to remove elastin selectively (Porter et al. 1977; Caldini et al. 1990) and stained as above. Unavoidable background staining enabled elastic fibres to be contextualized with respect to the rest of the extracellular matrix under polarized light.

Sections were viewed using an automated microscope (DM6000 B; Leica Microsystems, Wetzlar, Germany) attached to a digital imaging workstation (Q500MC; Leica Microsystems). The use of *z*-series composite images allowed improved visualization of fibres through the extent of the 30-μm section at high magnification (Smith & Fazzalari, 2005). These were produced by taking stacks of images at between 0.1- and 0.8-μm intervals at an objective magnification of 100× under phase contrast through the extent of the section thickness (QWin; Leica Microsystems), then merging them to produce a single *z*-projected image (ImageJ; National Institutes of Health, Bethesda, MD, USA). Binarizing and processing such images (Matlab; Mathworks, Natick, MA, USA) both facilitated the production of three-dimensional reconstructions of elastic fibre organization, and the overlay of polarized light images with elastic fibres, enabling close examination of elastic fibre and collagen fibril co-distribution.

Quantitation

Quantitation was limited to intralamellar zones of the anulus, as elastic fibre distribution was observed to be more isotropic here than in interlamellar zones. Additionally, quantitation was performed exclusively on transverse sections as this planar orientation most easily facilitated the regional analysis. Elastic fibres were quantified as the mean number intercepted by the lines of a 6×6 grid, normalized as the number of elastic fibres per 100 μm. To compare regional variations in fibre distribution, the mean results from sets of six fields taken within randomly selected representative collagen lamellae in the outer, middle and inner anulus of the anterolateral and posterolateral quadrants (a total of six regional zones, illustrated in Fig. 1) were calculated. Distinct radial locations were defined according to established differences in collagen lamella morphology which occur at increasing distances from the disc periphery (Cassidy et al. 1989; Marchand & Ahmed, 1990).

Statistical analyses were performed using SPSS software (SPSS Inc., Chicago, IL, USA). To determine the dependence of intralamellar elastic fibre density on circumferential location, paired Student *t*-tests were performed comparing overall mean intralamellar elastic fibre density between anterolateral and posterolateral quadrants, as well as at each of the three radial locations (outer, middle and inner). Single-factor analyses of variance (ANOVAs) were performed to determine if intralamellar elastic fibre density exhibited any significant dependence on radial location (three levels: inner, middle and outer) at each circumferential location (anterolateral and posterolateral). Where ANOVAs showed significant variation, *post-hoc* pairwise analysis applying

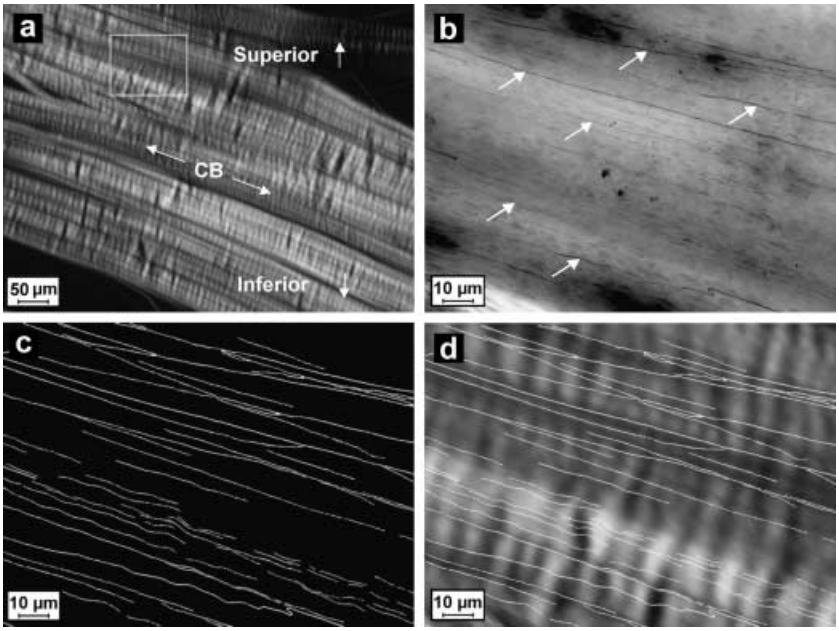

Fig. 2 Intralamellar elastic fibres and the surrounding matrix architecture of the outer anulus viewed in the lamellar plane. (a) Polarized light image depicting collagen fibril bundles (CB) in the outer anulus of a 40-year-old disc running at 30° to the transverse plane. (b) High-magnification, phase-contrast, *z*-series composite image in the region of image (a) indicated by the square, showing elastic fibres (examples indicated by arrows) running parallel to the collagen fibril bundles. (c) Binarized reconstruction of (b). (d) Elastic fibres in (c) are superimposed over a high-magnification, polarized-light view of the same region showing elastic fibre distribution relative to the collagen microarchitecture, including planar crimp.

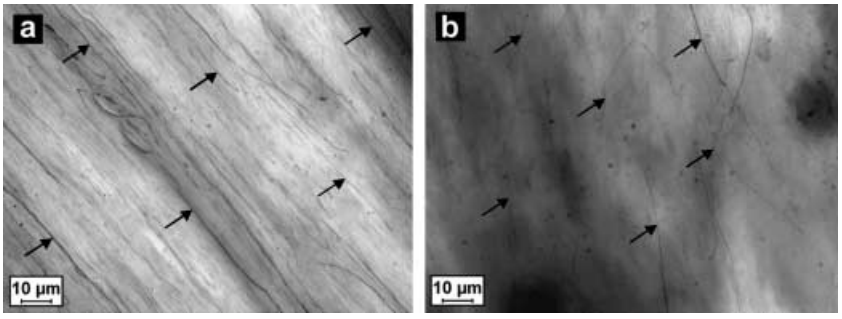

Fig. 3 Phase-contrast *z*-series composite images in the transverse plane depicting intralamellar elastic fibres in the posterolateral anulus of a 28-year-old disc. (a) Fibres in the outer anulus are numerous, parallel and tightly bound by the surrounding matrix. (b) Fibres in the inner anulus are fewer in number and more loosely aligned. Examples of elastic fibres are indicated by arrows in both images.

Bonferroni corrections was undertaken. *F*-tests were performed to compare variances. Significance for all tests was reported at a confidence level of 95%.

Results

Elastic fibre morphology in sections stained with resorcin-fuchsin compared favourably with that described in the literature (Yu et al. 2002, 2005). No fibres were observed in negative controls. Although elastic fibres could be observed under bright-field illumination, under phase contrast their visual clarity was enhanced.

In lamellar and transverse plane sections elastic fibres in intralamellar zones were observed aligned parallel to the collagen fibres (i.e. at angles of approximately 30° to the transverse plane). In interlamellar zones their architecture was more complex and highly anisotropic. By combining high-magnification polarized light and binarized phase contrast images, we were able to compare the arrangement of elastic fibres with the microarchitecture of the surrounding collagen matrix. Figure 2 shows the intralamellar zone of the outer anulus in the lamellar plane. Elastic fibres are not confined to the periphery of the collagen bundles, and appear to conform to the planar crimped pattern of the collagen fibrils. Similar zones viewed in the transverse plane (Fig. 3) illustrate that in the outer anulus, elastic fibres are straight and tightly packed within the surrounding matrix, and in the inner regions they are more loosely arranged. Figures 4 and 5 depict interlamellar zones orientated in the lamellar and transverse planes, respectively. Elastic fibres here form a complex inter-woven mesh branching out from the collagen bundles

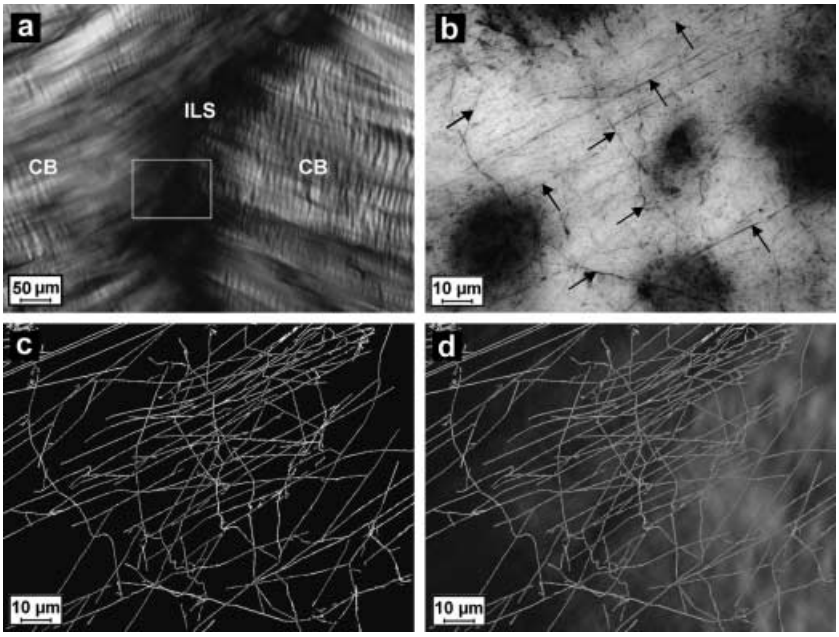

Fig. 4 Interlamellar elastic fibres and the surrounding matrix architecture viewed in the lamellar plane. (a) Polarized light image depicting an oblique cut through the interlamellar space (ILS) separating two consecutive collagen bundle lamellae (CB). (b) High-magnification, phase-contrast, *z*-series composite image in the region of image (a) indicated by the square, showing a complex meshwork of elastic fibres in the interlamellar space (examples indicated by arrows). (c) Binarized reconstruction of (b). (d) Elastic fibres in (c) are superimposed over a high-magnification, polarized-light view of the same region.

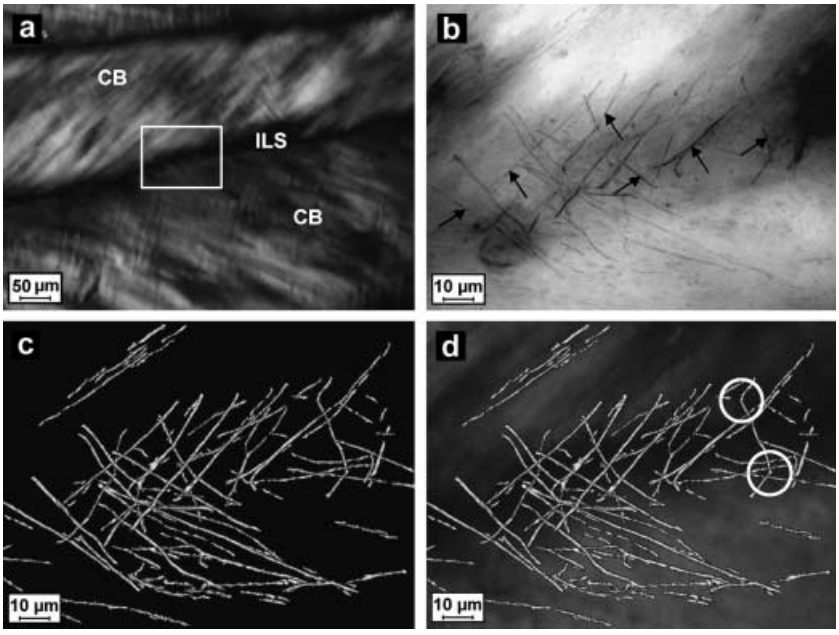

Fig. 5 Interlamellar elastic fibres and the surrounding matrix architecture viewed in the transverse plane. (a) Polarized light image depicting two collagen bundle lamellae (CB) separated by an interlamellar space (ILS). (b) High-magnification, phase-contrast, *z*-series composite image in the region of image (a) indicated by the square, showing a complex meshwork of elastic fibres (examples indicated by arrows) in the interlamellar space. (c) Binarized reconstruction of (b). (d) Elastic fibres in (c) are superimposed over a high-magnification, polarized-light view of the same region showing elastic fibre distribution relative to the collagen microarchitecture. The circles indicate fibre 'kinks' at the points of anchorage into the collagen bundles.

in the adjacent lamellae. Within these meshworks combinations of both large and very fine fibres were observed. An interesting observation was made in that a number of fibres were seen to 'kink' at their point of exit from the collagen bundle into the interlamellar space. This characteristic is illustrated by the circles in Fig. 5(d).

The images in Fig. 3 are representative of those used for the quantitative analysis. Individual results for each specimen are given in Table 2. Overall intralamellar elastic fibre density was significantly greater in the posterolateral region of the anulus than the anterolateral (AL = 6 ± 2, PL = 12 ± 4, $P = 0.002$, mean $\pm$ SD). Additionally, it was found that this circumferential variation was independent of radial location (Outer: AL = 9 ± 3, PL = 17 ± 6, $P = 0.001$; Middle: AL = 6 ± 2, PL = 12 ± 6, $P = 0.02$; Inner: AL = 4 ± 2, PL = 6 ± 3, $P = 0.007$) (Fig. 6).

Age	AL* Outer	AL Middle	AL Inner	PL* Outer	PL Middle	PL Inner	Overall
16	7 ± 3	4 ± 1	2 ± 1	15 ± 3	7 ± 4	4 ± 1	6 ± 5
28	13 ± 5	8 ± 2	3 ± 2	22 ± 8	17 ± 2	5 ± 3	10 ± 8
40	10 ± 2	8 ± 3	6 ± 2	21 ± 7	20 ± 9	10 ± 2	12 ± 8
54	11 ± 2	7 ± 2	4 ± 2	21 ± 4	15 ± 3	6 ± 4	11 ± 7
66	8 ± 4	6 ± 3	4 ± 2	8 ± 5	9 ± 4	4 ± 2	7 ± 4
76	10 ± 2	4 ± 2	7 ± 1	22 ± 7	15 ± 4	9 ± 3	11 ± 7
82	3 ± 2	4 ± 1	3 ± 1	12 ± 6	2 ± 1	4 ± 2	5 ± 5

Table 2 Intralamellar elastic fibre density – fibres per 100 μm (mean ± SD, $n \geq 6$)

*AL = anterolateral, PL = posterolateral.

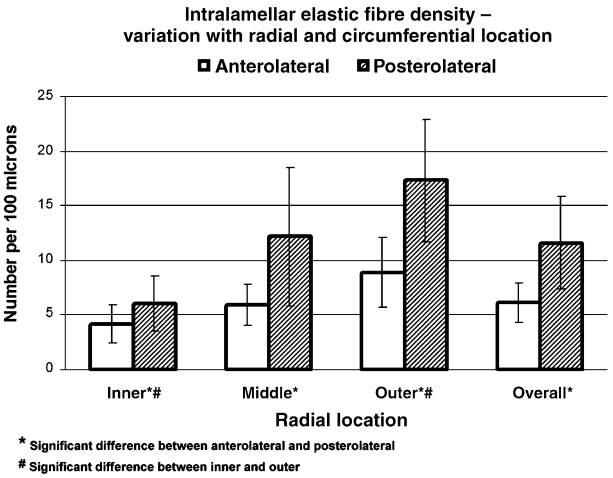

Fig. 6 Variations in intralamellar elastic fibre density with radial and circumferential location (mean ± SD, $n = 7$). Significance was detected between anterolateral and posterolateral (inner: $P = 0.02$, middle: $P = 0.007$, outer: $P = 0.001$, overall: $P = 0.002$), and between inner and outer (anterolateral: $P = 0.005$, posterolateral: $P = 0.002$).

An *F*-test revealed that elastic fibre density variance was significantly greater within the posterolateral region than the anterolateral ($P = 0.0003$).

Single factor analyses of variance demonstrated that significant variations in intralamellar elastic fibre density occurred with radial location in both anterolateral ($P = 0.006$) and posterolateral ($P = 0.002$) regions (Fig. 6). Pairwise Bonferroni-corrected *P*-values indicated that in both circumferential regions, the lamellae of the outer anulus had a significantly higher elastic fibre density than the lamellae of the inner anulus (AL: $P = 0.005$; PL: $P = 0.002$). No significant differences were detected between outer and middle (AL: $P = 0.09$; PL: $P = 0.2$), and middle and inner regions (AL: $P = 0.6$; PL: $P = 0.1$).

Owing to the small sample size, variations in elastic fibre density with age were not validated statistically, but a number of observations were made: an increasing trend between the ages of 16 and 40 was observed, followed by a marked decrease, with the exception of the 76-year-old, which had an overall fibre density higher than both the 60- and 82-year-olds.

Discussion

In this study, we have presented a quantitative description of the distribution of elastic fibres in the lamellae of each region in the human lumbar anulus fibrosus, and a multiplanar comparison of elastic fibre distribution patterns in the intralamellar and interlamellar zones. The unique methodology developed in this study allowed visualization of elastic fibres in the anulus at a level of detail not previously achieved.

Our study had several limitations: no assessment was made of the effect of distance from the endplates/vertebral bodies on elastic fibre density, although every effort was made to ensure sections were taken close to the mid-plane of the disc; aqueous fixation may have resulted in some distortion of lamellae, particularly in the inner anulus where glycosaminoglycan content is higher; and the effects of freezing and fixation on aspects of tissue morphology such as collagen fibril arrangement, and, consequently, elastic fibre arrangement, were not assessed, although the results of a previous study (Hickey & Hukins, 1979) suggest that such effects would be unlikely to influence our results significantly. Despite the robust imaging and quantitation methodology used, occasional heavy background staining may have resulted in some fine elastic fibres being obscured. A positive side-effect of this background staining, however, was that it enabled elastic fibres to be contextualized with respect to the rest of the extracellular matrix without the need for specific counterstaining.

A comparison of elastic fibre distribution patterns in intralamellar and interlamellar zones performed at

high magnification in the lamellar and transverse planes revealed distinct differences which suggest that elastic fibres have different mechanical roles at multiple levels of the anulus structural hierarchy. Within lamellae elastic fibres were observed to be closely associated with the surrounding collagen matrix, corresponding well to previous observations in the transverse and sagittal planes (Buckwalter et al. 1976; Johnson et al. 1984; Yu et al. 2002, 2005). Additionally, fibres appeared not to be confined to the collagen bundle peripheries. Planar crimping of fibrous collagen, as has been well documented (Cassidy et al. 1989), was clearly observed, particularly in lamellar plane sections. Elastic fibres appeared to conform to the crimp pattern of the surrounding collagen (Fig. 2), which suggests that they are not responsible for physically maintaining collagen crimp. Their close association, however, does suggest that the overall mechanical response of the matrix is a product of their mutual interaction, in addition to the interactions which may occur with proteoglycans.

In interlamellar zones, elastic fibres appeared in complex three-dimensional meshworks, which branched out from the adjacent collagen bundles into the interlamellar spaces. Combinations of both very large and very fine fibres were observed in these meshworks, suggesting the presence of all three elastic fibre types (mature, elaunin and oxytalan). Our results suggest that the complex linkages previously observed between collagen bundles in adjacent lamellae (Pezowicz et al. 2006) are indeed, at least partially, composed of elastic fibres. A number of fibres were seen to 'kink' at their point of exit from the collagen bundle into the interlamellar space, suggesting that the collagen bundles on either side of the interlamellar space into which the ends of elastic fibres are anchored have undergone relative movement, providing further evidence that these fibres function as mechancial links between lamellae.

Our quantitative analysis revealed intralamellar elastic fibre density to be significantly higher in the posterolateral region of the anulus than the anterolateral, and significantly higher in the outer regions of the anulus than the inner. To gain insights into why these differences in matrix composition may exist, we can consider the types of strains to which lamellae in different regions of the anulus are exposed during normal daily activity. During flexion, the posterior regions of the L3–L4 anulus experience positive axial strains of up to 60%, in contrast to the anterior regions, which experience just 3% in extension (Pearcy & Tibrewal, 1984). Additionally, in torsion, surface strains in the collagen fibre bundles of the posterolateral region exceed those in the anterior region by a factor of two to one (Stokes, 1987). Associated strains under the above loading conditions are greater in the collagen fibre bundles of the outer lamellae due to their relative distances from the axes of movement. We can hence hypothesize that elastic fibre density is positively correlated with the magnitudes of the tensile deformations experienced by different regions of the anulus under these loading conditions. An analysis of elastic fibre distribution in the flexor tendon, a comparable tissue, has suggested a similar correlation between elastic fibre distribution and strain magnitude (Ritty et al. 2002).

Although there are currently no experimental biomechanical data describing the functional roles played by elastic fibres in the mechanics of the intervertebral disc, their role has been described in a number of other comparable tissues (Karlinsky et al. 1976; Oakes & Bialkower, 1977; Oxlund et al. 1988; Brown et al. 1994; Lee et al. 2001). From the results of these studies we hypothesize that a primary function of elastic fibres in the anulus would be to facilitate the reversible distention of the collagen matrix in the locations they have been observed, i.e. both in the intralamellar zones between fibrils and bundles, and at interlamellar zones by connecting bundles in adjacent lamellae. We also hypothesize that elastic fibres may provide additional stiffness to the matrix at small stresses and strains, but that they would be unlikely to influence overall mechanical strength. These hypotheses could be tested in future biomechanical investigations.

The small number of specimens did not permit a statistically valid analysis to be conducted into elastic fibre density variation with age. Indeed, the large sample size that would be required for such a study and the time-consuming nature of the analyticial methodology used here placed it outside the scope of this project. However, a number of observations were made from the values presented in Table 2. Our results show an increasing trend between the ages of 16 and 40, followed by a marked decrease, with the exception of the 76-year-old, which had an overall fibre density higher than both the 60- and the 82-year-olds. A comparison of disc dimensions, disc morphological grades and vertebral body bone mineral densities for the 60-, 76- and 82-year-old specimens (Table 1) revealed that although all were assigned a grade of 3, the 76-year-old specimen had reduced height, as well as a significant

mismatch in bone mineral densities (T-scores) between the superior (L3) and inferior (L4) vertebral bodies. These factors could reasonably be expected to result in altered mechanical behaviour for this disc and, hence, matrix composition. Additionally, of these three the 76-year-old was the only female. If this specimen is excluded for the reasons described, our results appear broadly consistent with existing biochemical data showing that the elastin content of the anulus increases from birth until the age of 40, then steadily decreases (Olczyk, 1994). They are given added significance given recent findings that the tensile deformability of human lumbar discs peaks between the ages of 31 and 40, and subsequently decreases (Kurutz, 2006). Further work is required to confirm this apparent correlation.

In light of our findings, any decrease in elastic fibre density with age (Johnson et al. 1985; Olczyk, 1994) or pathology is of potential clinical significance, particularly with respect to those regions of the anulus subjected to the highest and most frequent deformations such as the posterior and posterolateral, which are also the most frequent sites for degenerative changes such as radiating tears (Vernon-Roberts et al. 1997). Additionally, weakening of those elastic fibres which bridge the interlamellar spaces could make the anulus more susceptible to delamination and the formation of circumferential lesions. Our findings also have important implications for the theoretical modelling of anulus fibrosus mechanics and may assist the development of accurate synthetic and biological tissue-engineered intervertebral disc replacements.

Acknowledgements

Funding for this project was provided by the National Health and Medical Research Council, the University of Adelaide and the Institute of Medical and Veterinary Science. Cadaveric material donated through the Royal Adelaide Hospital is gratefully acknowledged. We additionally acknowledge the assistance of Dr Bingkui Ma, Ms Gail Hermanis and Mr Arash Badiei.

References

Akhtar S, Davies JR, Caterson B (2005a) Ultrastructural immunolocalization of a-elastin and keratan sulfate proteoglycan in normal and scoliotic lumbar disc. *Spine* **30**, 1762–1769.

Akhtar S, Davies JR, Caterson B (2005b) Ultrastructural localization and distribution of proteoglycan in normal and scoliotic lumbar disc. *Spine* **30**, 1303–1309.

Barros EM, Rodrigues CJ, Rodrigues NR (2002) Aging of the elastic and collagen fibers in the human cervical interspinous ligaments. *Spine J* **2**, 57–62.

Brown RE, Butler JP, Rogers RA, Leith DE (1994) Mechanical connections between elastin and collagen. *Connect Tissue Res* **30**, 295–308.

Buckwalter JA, Cooper RR, Maynard JA (1976) Elastic fibers in human intervertebral discs. *J Bone Joint Surg Am* **58**, 73–76.

Bushell GR, Ghosh P, Taylor TF, Akeson WH (1977) Proteoglycan chemistry of the intervertebral disks. *Clin Orthop Relat Res* **129**, 115–123.

Caldini EG, Caldini N, De-Pasquale V, et al. (1990) Distribution of elastic system fibres in the rat tail tendon and its associated sheaths. *Acta Anat (Basel)* **139**, 341–348.

Cassidy JJ, Hiltner A, Baer E (1989) Hierarchical structure of the intervertebral disc. *Connect Tissue Res* **23**, 75–88.

Ebara S, Iatridis JC, Setton LA, Foster RJ, Mow VC, Weidenbaum M (1996) Tensile properties of nondegenerate human lumbar anulus fibrosus. *Spine* **21**, 452–461.

Elliott DM, Setton LA (2001) Anisotropic and inhomogeneous tensile behavior of the human anulus fibrosus: experimental measurement and material model predictions. *J Biomech Eng* **123**, 256–263.

Eyre DR (1979) Biochemistry of the intervertebral disc. *Int Rev Connect Tissue Res* **8**, 227–291.

Fujita Y, Duncan NA, Lotz JC (1997) Radial tensile properties of the lumbar annulus fibrosus are site and degeneration dependent. *J Orthop Res* **15**, 814–819.

Fujita Y, Wagner DR, Biviji AA, Duncan NA, Lotz JC (2000) Anisotropic shear behavior of the annulus fibrosus: effect of harvest site and tissue prestrain. *Med Eng Phys* **22**, 349–357.

Hickey DS, Hukins DW (1979) Effect of methods of preservation on the arrangement of collagen fibrils in connective tissue matrices: an x-ray diffraction study of annulus fibrosus. *Connect Tissue Res* **6**, 223–228.

Hickey DS, Hukins DW (1980) Relation between the structure of the annulus fibrosus and the function and failure of the intervertebral disc. *Spine* **5**, 106–116.

Hickey DS, Hukins DW (1981) Collagen fibril diameters and elastic fibres in the annulus fibrosus of human fetal intervertebral disc. *J Anat* **133**, 351–357.

Humzah MD, Soames RW (1988) Human intervertebral disc: structure and function. *Anat Rec* **220**, 337–356.

Johnson EF, Chetty K, Moore IM, Stewart A, Jones W (1982) The distribution and arrangement of elastic fibres in the intervertebral disc of the adult human. *J Anat* **135**, 301–309.

Johnson EF, Caldwell RW, Berryman HE, Miller A, Chetty K (1984) Elastic fibers in the anulus fibrosus of the dog intervertebral disc. *Acta Anat (Basel)* **118**, 238–242.

Johnson EF, Berryman H, Mitchell R, Wood WB (1985) Elastic fibres in the anulus fibrosus of the adult human lumbar intervertebral disc. A preliminary report. *J Anat* **143**, 57–63.

Karlinsky JB, Snider GL, Franzblau C, Stone PJ, Hoppin FG Jr (1976) In vitro effects of elastase and collagenase on mechanical properties of hamster lungs. *Am Rev Respir Dis* **113**, 769–777.

Kielty CM, Sherratt MJ, Shuttleworth CA (2002) Elastic fibres. *J Cell Sci* **115**, 2817–2828.

Kurutz M (2006) Age-sensitivity of time-related in vivo deformability of human lumbar motion segments and discs in pure centric tension. *J Biomech* **39**, 147–157.

Langrana NA, Edwards WT, Sharma M (1996) Biomechanical analysis of loads of the lumbar spine. In *The Lumbar Spine* (ed. Bell G), Vol. 1, pp. 163–181. Philadelphia: Saunders.

Lee TC, Midura RJ, Hascall VC, Vesely I (2001) The effect of elastin damage on the mechanics of the aortic valve. *J Biomech* **34**, 203–210.

Marchand F, Ahmed AM (1990) Investigation of the laminate structure of lumbar disc anulus fibrosus. *Spine* **15**, 402–410.

Miller PJ (1971) An elastin stain. *Med Lab Technol* **28**, 148–149.

Oakes VW, Bialkower B (1977) Biomechanical and ultrastructural studies on the elastic wing tendon from the domestic fowl. *J Anat* **123**, 369–387.

Oegema TR Jr (1993) Biochemistry of the intervertebral disc. *Clin Sports Med* **12**, 419–439.

Olczyk K (1994) Age-related changes of elastin content in human intervertebral discs. *Folia Histochem Cytobiol* **32**, 41–44.

Oxlund H, Andreassen TT (1980) The roles of hyaluronic acid, collagen and elastin in the mechanical properties of connective tissues. *J Anat* **131**, 611–620.

Oxlund H, Manschot J, Viidik A (1988) The role of elastin in the mechanical properties of skin. *J Biomech* **21**, 213–218.

Pearcy MJ, Tibrewal SB (1984) Lumbar intervertebral disc and ligament deformations measured in vivo. *Clin Orthop Relat Res* **191**, 281–286.

Pezowicz CA, Robertson PA, Broom ND (2006) The structural basis of interlamellar cohesion in the intervertebral disc wall. *J Anat* **208**, 317–330.

Porter K, Dooner JJ, Lopez A (1977) Further study of elastic fibers in human attached gingiva. *J Periodontol* **48**, 711–713.

Ritty TM, Ditsios K, Starcher BC (2002) Distribution of the elastic fiber and associated proteins in flexor tendon reflects function. *Anat Rec* **268**, 430–440.

Sheratt MJ, Baldock C, Haston JL, et al. (2003) Fibrillin microfibrils are stuff reinforcing fibres in compliant tissues. *J Mol Biol* **332**, 183–193.

Skaggs DL, Weidenbaum M, Iatridis JC, Ratcliffe A, Mow VC (1994) Regional variation in tensile properties and biochemical composition of the human lumbar anulus fibrosus. *Spine* **19**, 1310–1319.

Smith LJ, Fazzalari NL (2005) Elastic fibre network architecture in the human lumbar anulus fibrosus. In *Proceedings of the 29th Annual Meeting of the Matrix Biology Society of Australia and New Zealand, Victor Harbor, Australia* (eds Byers S, Gibson MA), pp. 44. Parkville: Matrix Biology Society of Australia & New Zealand.

Stokes IA (1987) Surface strain on human intervertebral discs. *J Orthop Res* **5**, 348–355.

Szirmai J (1970) Structure of the intervertebral disc. In *Chemistry and Biology of the Intercellular Matrix* (ed. Balazs E), Vol. 3, pp. 1297–1308. London: Academic Press.

Thompson JP, Pearce RH, Schechter MT, Adams ME, Tsang IK, Bishop PB (1990) Preliminary evaluation of a scheme for grading the gross morphology of the human intervertebral disc. *Spine* **15**, 411–415.

Vernon-Roberts B, Fazzalari NL, Manthey BA (1997) Pathogenesis of tears of the anulus investigated by multiple-level transaxial analysis of the T12–L1 disc. *Spine* **22**, 2641–2646.

Yu J, Winlove PC, Roberts S, Urban JP (2002) Elastic fibre organization in the intervertebral discs of the bovine tail. *J Anat* **201**, 465–475.

Yu J, Fairbank JC, Roberts S, Urban JP (2005) The elastic fiber network of the anulus fibrosus of the normal and scoliotic human intervertebral disc. *Spine* **30**, 1815–1820.